Robust Control for PWM-Based DC–DC Buck Power Converters With Uncertainty Via Sampled-Data Output Feedback

Chuanlin Zhang, Junxiao Wang, Shihua Li, *Senior Member, IEEE*, Bin Wu, and Chunjiang Qian, *Senior Member, IEEE*

***Abstract*—This paper investigates the sampled-data output feedback control problem for dc–dc buck power converters taking consideration of components uncertainties. A reduced-order observer and a robust output feedback controller, both in the sampled-data form, have been explicitly constructed with strong robustness in the presence of uncertain parameters. A delicate stability analysis process is presented to show that, by carefully selecting the design gains and the tunable sampling period, the output voltage of the hybrid closed-loop dc–dc buck converter system will globally asymptotically tend to the desired value even though the separation principle is out of reach and the controller is only switched at the sampling points. The proposed controller consists of a set of linear difference equations which will lead to direct and easier digital implementation. Numerical simulations and experimental results are shown to illustrate the performance of the proposed control scheme.**

***Index Terms*—DC–DC buck converters, output feedback control, reduced-order observer, sampled-data control, uncertainty attenuation.**

I. Introduction

DC–DC switched power converters, which are employed to adapt energy sources to the load requirements (or vice versa), are intensively used in direct current (DC) supply applications [1]–[3]. These devices present several challenges regarding their control issue since modern electronic systems such as computer systems, communication equipments, medical instruments, etc. deeply require high-quality, lightweight, reliable, adaptive, and efficient power supplies [4]–[10]. Early control efforts for these systems are contributed to the linear control methods based on linearized models [11], but it is clear that those control performances deteriorate under various disturbances in the dc–dc converter circuit. Later research results are devoted to nonlinear control strategies which are frequently studied as applications into different types of dc–dc converters in the literature, such as backstepping control [12], [13], adaptive control [14], model predictive control [15] and sliding mode control [16]–[19], fuzzy logic control [20], optimal control [21], [22], time-domain design [23], etc.

As is well known that dc–dc converters are typical nonlinear time-varying systems, but the system uncertainties are commonly neglected in the controller design. From a practical point of view, the magnetic characteristics of some components are actually uncertain and nonlinear especially in the presence of large magnetic flux density in the ferromagnetic core in the circuit as studied in [13], [24], and [25]. On the other hand, the parameter uncertainties in system models are inevitable in practical control problems caused by modeling errors, uncertain sensor measurement, different operating circumstances, and so on [26]–[28]. Hence, high efficient controllers which pursue smaller steady-state error, faster dynamical response, lower overshoot, and milder noise susceptibility are deeply needed. Besides these common requirements, the closed-loop control performance of the converter system should also perform good uncertainty attenuation ability when affected by uncertainties in its involved components or by input/output disturbances.

Comparing to various results aforementioned focusing on the design of state-feedback control laws for dc–dc power converters, fewer attentions are paid to the output feedback control strategies which utilize a sensor-less observer to reconstruct the current or voltage states. Whereas current-mode approaches are extensively studied by the power electronics engineers [29], in which current sensing in the state feedback is mandatory. In addition, the sensing procedures always suffer from noise, since in some cases such as in peak current control, the current waveform must be sensed accurately [30]. Therefore, a plain output-feedback approach is of interest in certain cases, in which a simple control is required while the sensing of all the states in the dc–dc converter is not easy to be reached. Moreover, output feedback control strategy distinguishes itself to its state feedback control counter-case mainly exists on its reliable and cost reducible features. It is depicted in [31] that the sensor-less control method has significant advantages over both conventional peak and average current-mode control techniques in noise susceptibility and dynamic range, in both continuous

Manuscript received September 27, 2013; revised December 10, 2013; accepted January 7, 2014. Date of publication January 13, 2014; date of current version August 26, 2014. This work is supported in part by Natural Science Foundation of China (61074013), the Science Foundation for Distinguished Young Scholars of Jiangsu Province (BK20130018), the Program for New Century Excellent Talents in University (NCET-10-0328). Recommended for publication by Associate Editor J. R. Rodriguez.

C. Zhang, J. Wang, S. Li, and B. Wu are with the School of Automation, Southeast University, Key Laboratory of Measurement and Control of CSE, Ministry of Education, Nanjing 210096, China (e-mail: clzhangseu@gmail.com; wangjunxiao19860128@126.com; lsh@seu.edu.cn; wubinauto@126.com).

C. Qian is with the Department of Electrical and Computer Engineering, University of Texas at San Antonio, San Antonio, TX 78249 USA (e-mail: Chunjiang.Qian@utsa.edu).

Digital Object Identifier 10.1109/TPEL.2014.2299759

mode and discontinuous mode. And later in [32], a robust adaptive output feedback control law is addressed to regulating the output voltage of dc–dc series resonant converters.

The objective of this paper is to design a global robust tracking law for the dc–dc buck converters with consideration of the uncertainties presented with the capacitance and inductance via sampled-data output feedback, which provides direct digital implementation. Different from the typical direct discretization method whose controller design is based on the approximation discrete-time system model [33], [34], this paper uses the nonlinear emulation method [35]–[38] to take fully advantages of the nonlinear recursive design techniques [39], [40] along with the output domination technique [41]. To this direction, first a novel discrete-time reduced-order observer is constructed to observe the unmeasurable state in the sampling points. Different from conventional full-dimensional high-gain observers [42], [43], the proposed robust reduced-order observer is still effective under the perturbation from the system uncertainties. Then by extending the output domination approach and restraining the state growth under a zero-order-hold input, a delicate stability analysis is presented to show that with a carefully selected sampling period, the global attractivity of the hybrid closed-loop system, while the sampled-data controller is dormant during the sampling instants can be guaranteed. Comparing to the previous related results concerning on the robust control issue for dc–dc buck converters, the main contributions of this paper exist on the following three aspects:

1) In the presence of uncertain parameters, the proposed sensor-less control design adopts a sampled-data reduced-order observer, rather than a full-order observer, to estimate the unmeasurable state information in the sampling point; hence, the implementation cost is reduced.
2) The explicit design procedure of the control law builds a detailed analytic relationship among the hybrid closed-loop system performance, the selection of the scaling gains, and the calculation of the sampling period.
3) The proposed control scheme exists on the fact that it consists of a set of linear difference equations without losing its high-precision tracking performance and strong robustness; hence, it provides the engineers direct and easier implementation via digital computers.

The paper is organized as follows. Section II introduces the system model and the problem statement. Section III gives the explicit control law construction procedure. In Section IV, the numerical simulations and experimental results will show the effectiveness of the proposed controller. And, then a conclusion and a reference list end the paper.

II. System Model Description and Problem Statement

Fig. 1 shows a typical dc–dc switched buck power converter circuit, where i_L is the average inductor current, and v_o the average output capacitor voltage, R is the load resistance of the circuit, $V_{\rm in}$ is a dc input voltage source, the duty ratio function $\mu \in [0,1]$ represents the control signal and the desired output voltage is depicted by V_d. The average system model for dc–dc buck power converter, as described in [44] and [18], can be written as follows:

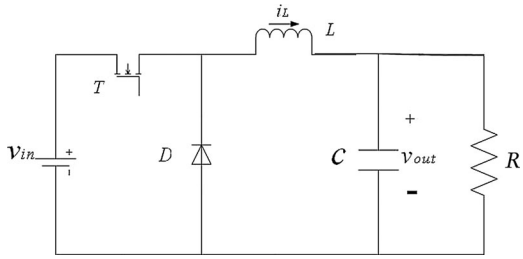

Fig. 1. DC–DC Buck converter circuit.

$$\begin{aligned}\frac{di_L}{dt} &= \frac{1}{L}\mu V_{\rm in} - \frac{1}{L}v_o \\ \frac{dv_o}{dt} &= \frac{1}{C}i_L - \frac{1}{CR}v_o. \end{aligned} \tag{1}$$

As discussed in the introduction that the involved components always subject to uncertainties and may be nonlinear in practical situations, to cover a more general control result for the dc–dc buck power converters, this paper takes consideration of the case that the involved components L, C may be time-varying, not fixed. In an analytical way, L and C can be formulated with uncertainties as the following form

$$\frac{1}{L} = \theta_L(t)\frac{1}{L_0}, \quad \frac{1}{C} = \theta_C(t)\frac{1}{C_0} \tag{2}$$

where L_0, C_0 are exactly known nominal values of the capacitance and inductance, respectively. $\theta_L(t), \theta_C(t)$ represent the time-varying uncertain nonlinear parameters which satisfy the following assumption.

Assumption 2.1: There exist positive constants $\bar{\theta}_L$, $\underline{\theta}_L$, $\bar{\theta}_C$, $\underline{\theta}_C$, $\bar{\theta}_C^*$, such that the following inequalities hold:

$$\begin{aligned}\underline{\theta}_L \le \theta_L(t) \le \bar{\theta}_L \\ \underline{\theta}_C \le \theta_C(t) \le \bar{\theta}_C \\ \left|\frac{d\theta_C(t)}{dt}\right| \le \bar{\theta}_C^*. \end{aligned}$$

Remark 2.1: In practice, the inductance and capacitance in the circuit may continually change subject to uncertain outer circumstances or other disturbances, such as the temperature, magnetic coil saturation, production materials, etc. [13], [25]. Only the nominal (approximate) values of L and C in a circuit are assumed to be available, namely L_0 and C_0, but their varying amplitudes are relatively milder compared to there nominal values. This fact implies the formulation of the form (2) as well as Assumption 2.1 are quit reasonable.

With the presence of the uncertain parameters, (1) can be modified as the following form:

$$\begin{aligned}\frac{di_L}{dt} &= \theta_L(t)\frac{1}{L_0}\mu V_{\rm in} - \theta_L(t)\frac{1}{L_0}v_o \\ \frac{dv_o}{dt} &= \theta_C(t)\frac{1}{C_0}i_L - \theta_C(t)\frac{1}{C_0R}v_o. \end{aligned} \tag{3}$$

In this paper, the authors are aiming to solve the global tracking control problem for the modified uncertain dc–dc buck converter (3) via sampled-data output feedback. Now, we present the main theorem of this paper whose proof will be introduced in Section III.

Theorem 2.1: Under Assumption 2.1, there exist a series of appropriate constant gains M, N, β_1, β_2 and a tunable sampling period T, such that the following robust sampled-data output feedback control law with a discrete-time reduced-order observer

$$\hat{z}(t_{k+1}) = e^{-MNT}\hat{z}(t_k) + N(1-e^{-MNT})y(t_k) \tag{4}$$

$$\mu(t) = \big(V_d - M^2\beta_2\big(\hat{z}(t_k) + (N+\beta_1)y(t_k)\big)\big)/V_{\text{in}}, \quad t \in [t_k, t_{k+1}), \quad t_k = kT, k \in \mathbb{N} \tag{5}$$

where $\hat{z}(t_k)$ is the estimated state denoted by $\hat{z}(t_k) = \hat{x}_2(t_k) - Ny(t_k)$, and $y(t_k) = v_o(t_k) - V_d$ represents the output signal, will render the output voltage v_o in the uncertain dc–dc buck converter system (3) globally asymptotically track the desired output voltage value V_d.

Remark 2.2: In most practical implementation processes, it is common that the continuous-time controllers can be discretized directly which exists on the fact that the closed-loop system performance can always be guaranteed while the sampling frequency is fast enough. And, it is clear that the closed-loop system performance deteriorates with respect to an increasing sampling period. However from a theoretical point of view, there are few results concerning on the feasibility analysis of such a procedure. In other words, the formulated restrictions of the sampling period T (i.e., the selectable margin of T), the relationship between T and control gains or other involved parameters and how the selection of T affects the controlled system performance are actually not clear. Aiming to narrow the gap between the control theory and control applications, this paper presents the engineers a sampled-data control law design where explicit formulas to select the control gains and the tunable sampling period based on a detailed stability analysis for the hybrid closed-loop uncertain DC-DC buck converter system are presented. Hence, it will be a helpful guideline for direct digital implementation.

Remark 2.3: In most of the existing results concerning on the sensor-less control problem for dc–dc power converters, full-order observers are always utilized which rely on the fact that the system information should be precisely known. As a matter of fact, the unknown parameters $\theta_C(t)$ and $\theta_L(t)$ in system (3) will be an obstacle when designing observers which should utilize the exact information from the original system. Even those observers designed neglecting the system uncertainties are sometimes still useful in the practical cases, but the robustness of the output feedback controllers cannot be guaranteed. In this paper, utilizing a novel sampled-data reduced-order observer of the form (4), which performs strong robustness in the presence of those uncertain parameters, a global robust sampled-data output feedback controller in the form of (5) can be explicitly designed.

III. Sampled-Data Output Feedback Control Law Design

A. Explicit Design Procedure

In this section, an explicit design procedure divided into several steps is provided. First, a change of coordinates is introduced to bring a scaling gain into the system. Second, we construct a discrete-time reduced-order observer to estimate the unmeasurable state information in the sampling point. Then, a state-feedback control law are designed using a recursive design technique [39]. Followed by the stability analysis for the controlled hybrid closed-loop system, an explicit formula of the assignment of the gains and the computation of the tunable sampling period are given in the last step.

Step 1: Change of Coordinates

With the following change of coordinates:

$$y = x_1 = v_o - V_d, x_2 = \dot{x}_1/M = \dot{v}_o/M, u = (\mu V_{\text{in}} - V_d)/M^2$$

where the constant scaling gain $M \geq 1$ will be determined later, (3) can be rewritten as

$$\begin{aligned}
\dot{x}_1(t) &= Mx_2(t)\\
\dot{x}_2(t) &= \theta_L(t)\theta_C(t)\frac{M}{L_0C_0}u(t) - \frac{1}{M}\theta_L(t)\theta_C(t)\frac{1}{L_0C_0}x_1(t)\\
&\quad - \left(\frac{\theta_C(t)}{C_0R} - \frac{\dot{\theta}_C(t)}{\theta_C(t)}\right)x_2(t)\\
y(t) &= x_1(t).
\end{aligned} \tag{6}$$

Step 2: Sampled-Data Reduced-Order Observer Design

In what follows, a reduced-order observer for system, (6) will be built using the sampled-data information from the output in the sampling point $y(t_k) = x_1(t_k)$, and the continuous-time state $x_2(t)$ defined in the time region $t \in [t_k, t_{k+1})$

$$\dot{\hat{z}}(t) = -MN\hat{z}(t) - MN^2y(t_k) \tag{7}$$

where N is a constant gain to be assigned later and $\hat{x}_2(t) = \hat{z}(t) + Ny(t)$.

Integrating the continuous-time observer (7) from t_k to t_{k+1}, one can conclude that (7) will generate the same $\hat{z}(t_{k+1})$ at the sampling point t_{k+1} for the same initial condition with the following sampled-data observer

$$\begin{aligned}
\hat{z}(t_{k+1}) &= e^{-MNT}\hat{z}(t_k) + \int_0^T e^{-MNs}dsMN^2y(t_k)\\
&= e^{-MNT}\hat{z}(t_k) + N(1-e^{-MNT})y(t_k).
\end{aligned} \tag{8}$$

Thus, in the remainder of this paper, we will use the continuous-time form of the observer for the convenience of stability analysis.

Denote the error $e(t) = z(t) - \hat{z}(t)$, where $z(t) = x_2(t) - Ny(t)$. We can deduce from (6) and (7) that the error dynamics are

$$\begin{aligned}
\dot{e}(t) &= -MNe(t) + \theta_L(t)\theta_C(t)\frac{M}{L_0C_0}u(t)\\
&\quad - \frac{1}{M}\theta_L(t)\theta_C(t)\frac{1}{L_0C_0}x_1(t)
\end{aligned}$$

$$- \left(\frac{\theta_C(t)}{C_0 R} - \frac{\dot{\theta}_C(t)}{\theta_C(t)} \right) x_2(t) - MN^2(y(t) - y(t_k)),$$
$$t \in [t_k, t_{k+1}). \tag{9}$$

Construct a positive definite and proper Lyapunov function $W(e(t)) = \frac{1}{2}e^2(t)$. The derivative of $W(e(t))$ along the error dynamics (9) satisfies the following inequality

$$\dot{W}(e(t)) \le -MNe^2(t) + \theta_L(t)\theta_C(t)\frac{M}{L_0C_0}|e(t)\|u(t)|$$
$$+ |e(t)| \left| \theta_L(t)\theta_C(t)\frac{x_1(t)}{ML_0C_0} + \left(\frac{\theta_C(t)}{C_0R} - \frac{\dot{\theta}_C(t)}{\theta_C(t)} \right) x_2(t) \right|$$
$$+ MN^2|e(t)\|y(t) - y(t_k)|, t \in [t_k, t_{k+1}). \tag{10}$$

Step 3: Linear Continuous-Time State Feedback Control Law Design

Choose a Lyapunov function which is positive definite and proper $V_1(x_1(t)) = \frac{1}{2}x_1^2$. The derivative of $V_1(x_1(t))$ along system (1) is

$$\dot{V}_1(x_1(t)) = Mx_1(t)x_2(t)$$
$$= Mx_1(t)x_2^*(t) + Mx_1(t)(x_2(t) - x_2^*(t)). \tag{11}$$

The virtual controller is chosen as $x_2^*(t) = -\beta_1 x_1(t)$, where $\beta_1 \ge 1$. Equation (6) becomes

$$\dot{V}_1(x_1(t)) \le -Mx_1^2(t) + M|x_1(t)\|x_2(t) - x_2^*(t)|. \tag{12}$$

Denote $\xi_1(t) = x_1(t)$ and $\xi_2(t) = x_2(t) - x_2^*(t)$. Construct a positive definite and proper Lyapunov function

$$V_2(x_1(t), x_2(t)) = \frac{1}{2}\left(\xi_1^2(t) + \xi_2^2(t)\right).$$

One can easily calculate the derivative of $V_2(x_1(t), x_2(t))$ along system (1) which satisfies

$$\dot{V}_2 \le -M\xi_1^2(t) + M|\xi_1(t)\xi_2(t)| + \theta_L(t)\theta_C(t)\frac{M}{L_0C_0}\xi_2(t)u(t)$$
$$+ \theta_L(t)\theta_C(t)\frac{1}{M}\frac{1}{L_0C_0}|\xi_1(t)\|\xi_2(t)|$$
$$+ \left| \frac{\theta_C(t)}{C_0R} - \frac{\dot{\theta}_C(t)}{\theta_C(t)} \right| x_2(t)\|\xi_2(t)| + M\beta_1|x_2(t)\|\xi_2(t)|. \tag{13}$$

With the help of Lemma A.1, we have

$$M|\xi_1(t)\xi_2(t)| \le \frac{M}{4}\xi_1^2(t) + M\xi_2^2(t). \tag{14}$$

With Assumption 2.1 in mind and notice that $M > 1$, by utilizing Lemma A.1, there exists a positive constant $d_1 > 0$, such that the following inequality holds:

$$\theta_L(t)\theta_C(t)\frac{1}{M}\frac{1}{L_0C_0}|\xi_1(t)\|\xi_2(t)| + \left| \frac{\theta_C(t)}{C_0R} - \frac{\dot{\theta}_C(t)}{\theta_C(t)} \right| x_2(t)\|\xi_2(t)|$$
$$\le \frac{\bar{\theta}_L\bar{\theta}_C}{L_0C_0}|\xi_1(t)\|\xi_2(t)| + \left(\left| \frac{\bar{\theta}_C}{C_0R} \right| + \left| \frac{\bar{\theta}_C^*}{\underline{\theta}_C} \right| \right) |\xi_2(t) + \beta_1\xi_1(t)\|\xi_2(t)|$$
$$\le \frac{1}{4}d_1(\xi_1^2(t) + \xi_2^2(t)). \tag{15}$$

Similarly, one can also have

$$M\beta_1|x_2(t)\|\xi_2(t)| \le M\beta_1|\xi_2(t) + \beta_1\xi_1(t)\|\xi_2(t)|$$
$$\le \frac{M}{4}\xi_1^2(t) + d_2M\xi_2^2(t) \tag{16}$$

where $d_2 > 0$ is a constant.

Substituting (14), (15), and (16) into (13) yields

$$\dot{V}_2 \le -\frac{1}{2}(M - \frac{d_1}{2})\xi_1^2(t) + \left((1 + d_2)M + \frac{d_1}{4}\right)\xi_2^2(t)$$
$$+ \theta_L(t)\theta_C(t)\frac{M}{L_0C_0}\xi_2(t)u_c(t)$$
$$+ \theta_L(t)\theta_C(t)\frac{M}{L_0C_0}|\xi_2(t)\|u(t) - u_c(t)|, t \in [t_k, t_{k+1}). \tag{17}$$

We choose the following continuous-time state-feedback controller

$$u_c(t) = -\beta_2\xi_2(t) = -\beta_2(x_2(t) + \beta_1 x_1(t)),$$
$$\beta_2 \ge \frac{(d_2 + \frac{3}{2})L_0C_0}{\underline{\theta}_L\underline{\theta}_C}. \tag{18}$$

With Assumption 2.1 in mind, substituting (18) into (17) yields

$$\dot{V}_2 \le -\frac{1}{2}\left(M - \frac{d_1}{2}\right)(\xi_1^2(t) + \xi_2^2(t))$$
$$+ \theta_L(t)\theta_C(t)\frac{M}{L_0C_0}|\xi_2(t)\|u(t) - u_c(t)|, t \in [t_k, t_{k+1}). \tag{19}$$

Step 4: Sampled-Data Output Feedback Controller Design

With the sampled-data observer (8), after a discretization process for the continuous-time controller (18) and by replacing the unmeasurable states with the estimated information in the sampling point t_k, the sampled-data output feedback controller for the dc–dc buck converter can be constructed as

$$u(t) = u(t_k) = -\beta_2(\hat{x}_2(t_k) + \beta_1 x_1(t_k)), \quad t \in [t_k, t_{k+1}), \tag{20}$$

i.e., the duty ration $\mu(t)$ as the control signal in the sampled-data form is formulated by

$$\mu(t) = \left(V_d - M^2\beta_2\left(\hat{z}(t_k) + (N + \beta_1)y(t_k)\right)\right)/V_{\text{in}},$$
$$t \in [t_k, t_{k+1}). \tag{21}$$

Denote $\mathcal{Z}(t) = (x_1(t), x_2(t), \hat{z}(t))^T$ and construct a Lyapunov function $U(\mathcal{Z}(t)) = V_2(x_1(t), x_2(t)) + W(e(t))$. Combining (12) and (5) together yields

$$\dot{U}(\mathcal{Z}(t))$$
$$\le -\frac{1}{2}(M - \frac{d_1}{2})(\xi_1^2(t) + \xi_2^2(t)) - MNe^2(t)$$
$$+ |e(t)| \left| \frac{1}{M}\theta_L(t)\theta_C(t)\frac{1}{L_0C_0}x_1(t) + \left(\frac{\theta_C(t)}{C_0R} - \frac{\dot{\theta}_C(t)}{\theta_C(t)} \right) x_2(t) \right|$$
$$+ \theta_L(t)\theta_C(t)\frac{M|e(t)\|u(t)|}{L_0C_0} + \frac{M\theta_L(t)\theta_C(t)}{L_0C_0}|\xi_2(t)\|u(t) - u_c(t)|$$
$$+ MN^2|e(t)\|y(t) - y(t_k)|, \quad t \in [t_k, t_{k+1}). \tag{22}$$

The following propositions whose proofs can be found in the Appendix will help us to estimate the items on the right hand of (22) using mathematical restraining technique.

Proposition 3.1: There exist constants $d_3 > 0$, $d_4 > 0$, such that the following inequality holds:

$$\begin{aligned}&\theta_L(t)\theta_C(t)\frac{M}{L_0C_0}|e(t)\|u(t)| + \frac{M\theta_L(t)\theta_C(t)}{L_0C_0}|\xi_2(t)\|u(t)-u_c(t)|\\ &\le \frac{M}{4}(\xi_1^2(t)+\xi_2^2(t)) + Md_3e^2(t)\\ &\quad + d_4MN(|\xi_2(t)|+|e(t)|)\cdot\|\mathcal{Z}(t)-\mathcal{Z}(t_k)\|, t\in[t_k,t_{k+1}).\end{aligned} \tag{23}$$

Proposition 3.2: There exists constants $\gamma > 0$, $\bar{\gamma} > 0$, such that the following inequality holds:

$$\|\mathcal{Z}(t)-\mathcal{Z}(t_k)\| \le \bar{\gamma}\sqrt{U(\mathcal{Z}(t_k))}\left(e^{\gamma M(t-kT)}-1\right), \quad t\in[t_k,t_{k+1}). \tag{24}$$

Noting that $M > 1$, one can also obtain the following estimation with Assumption 2.1 and Lemma A.1:

$$\begin{aligned}&|e(t)|\left|\frac{1}{M}\theta_L(t)\theta_C(t)\frac{1}{L_0C_0}x_1(t)+\left(\frac{\theta_C(t)}{C_0R}-\frac{\dot{\theta}_C(t)}{\theta_C(t)}\right)x_2(t)\right|\\ &\le |e(t)|\left(\frac{1}{M}\bar{\theta}_L\bar{\theta}_C\frac{1}{L_0C_0}|\xi_1(t)| + \left(\frac{\bar{\theta}_C}{C_0R}+\frac{\bar{\theta}_C^*}{\underline{\theta}_C}\right)|\xi_2(t)+\beta_1\xi_1(t)|\right)\\ &\le \frac{1}{4}d_5\left(\xi_1^2(t)+\xi_2^2(t)+e^2(t)\right)\end{aligned} \tag{25}$$

with a constant $d_5 > 0$.

Using Propositions 3.1–3.2 and substituting (25) into (22) yields

$$\begin{aligned}&\dot{U}(\mathcal{Z}(t))\\ &\le -\frac{1}{4}(M-d_1-d_5)(\xi_1^2(t)+\xi_2^2(t))\\ &\quad -\frac{1}{4}\left(4M(N-d_3)-d_5\right)e^2(t)\\ &\quad +\left(d_4MN(|e(t)|+|\xi_2(t)|)+MN^2|e(t)|\right)\|\mathcal{Z}(t)-\mathcal{Z}(t_k)\|\\ &\le -\frac{1}{4}(M-d_1-d_5)(\xi_1^2(t)+\xi_2^2(t))\\ &\quad -\frac{1}{4}\left(4M(N-d_3)-d_5\right)e^2(t)\\ &\quad +d_6MN^2\bar{\gamma}\sqrt{U(\mathcal{Z}(t))}\sqrt{U(\mathcal{Z}(t_k))}\left(e^{\gamma M(t-kT)}-1\right),\\ &t\in[t_k,t_{k+1})\end{aligned} \tag{26}$$

where $d_6 > 0$ is a constant.

Choose the observer gain N and the scaling gain M as the following form:

$$N \ge d_3+\frac{1}{4}, \quad M \ge \max\{d_1+d_5+2r^*,1\} \tag{27}$$

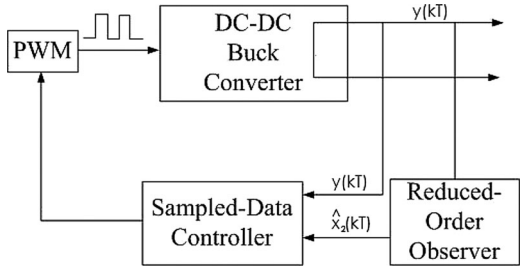

Fig. 2. Structure of dc–dc buck converters based on sampled-data output feedback controller.

where r^* is any positive constant and the tunable sampling period T should satisfy the following formula:

$$T < \frac{1}{\gamma M}\ln\left(r^*+\frac{1}{d_6MN^2\bar{\gamma}}\right). \tag{28}$$

With the choices of (27) and (28), now we are ready to prove Theorem 2.1.

B. Proof of Theorem 2.1

With the help of (27), one can rewrite (26) as

$$\begin{aligned}\dot{U}(\mathcal{Z}(t)) &\le -r^*U(\mathcal{Z}(t)) + d_6MN^2\bar{\gamma}\sqrt{U(\mathcal{Z}(t))}\sqrt{U(\mathcal{Z}(t_k))}\\ &\quad\times\left(e^{\gamma M(t-kT)}-1\right), t\in[t_k,t_{k+1}).\end{aligned} \tag{29}$$

Define $\zeta(t) = \frac{\sqrt{U(\mathcal{Z}(t))}}{\sqrt{U(\mathcal{Z}(t_k))}}$. Equation (29) equals to the following inequality:

$$\begin{aligned}\dot{\zeta}(t) &\le -\frac{r^*}{2}\zeta(t)+\frac{d_6MN^2\bar{\gamma}}{2}\left(e^{\gamma M(t-kT)}-1\right)\\ &\le -\frac{r^*}{2}\zeta(t)+\frac{d_6MN^2\bar{\gamma}}{2}\left(e^{\gamma MT}-1\right), \quad t\in[t_k,t_{k+1}).\end{aligned} \tag{30}$$

Solving the above inequality together with the fact that $\zeta(t_k) = 1$, one can have

$$\begin{aligned}\zeta(t_{k+1}) &\le d_6MN^2\bar{\gamma}\left(e^{\gamma MT}-1\right)\left(1-e^{-r^*T/2}\right)\\ &\quad +e^{-r^*T/2} := \rho(T).\end{aligned} \tag{31}$$

For a fixed sampling period T satisfying (28), it is clear that $\rho(T) < 1$, which leads to

$$\zeta(t_{k+1}) \le \rho(T) \Rightarrow U(\mathcal{Z}(t_{k+1})) \le \rho(T)U(\mathcal{Z}(t_k)). \tag{32}$$

Hence, $V\left(\mathcal{Z}(t_k)\right)$ converges to zero as k goes to infinity. As a conclusion, the closed-loop hybrid system (1), (8), and (15) is globally asymptotically stable. This completes the proof of Theorem 2.1.

Remark 3.1: Fig. 2 depicts the implementation structure of dc–dc buck converters with the proposed sampled-data output feedback controller (4)–(5). What is worth pointing out here is that the proposed sampled-data controller of the form (5) consists of a set of linear difference equations which is not losing its high precision tracking performance and robustness; hence, it will lead to direct and simpler digital implementation.

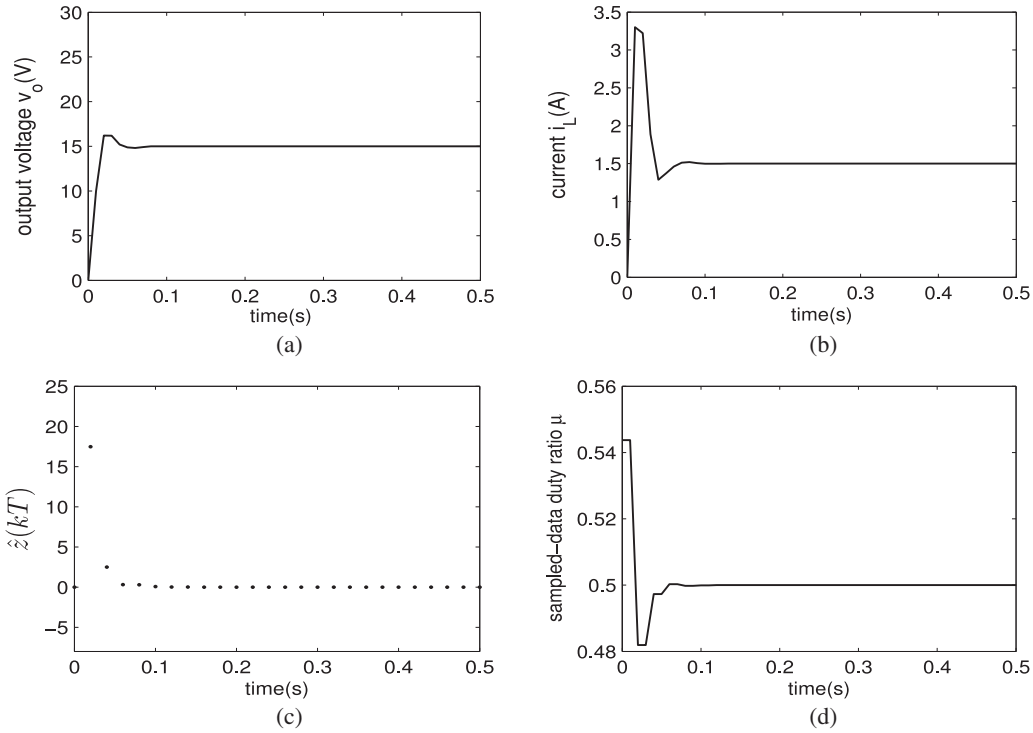

Fig. 3. Response curves of the system states under sampled-data output control law (5) with the presence of uncertain parameters. (a) Output voltage v_o. (b) Current i_L. (c) $\hat{z}(kT)$ generated from the observer (4). (d) Time history of the sampled-data control signal, duty ratio $\mu(t)$.

Remark 3.2: The main challenges in the above controller design exist due to the following two aspects. First, noting that the existing results rely on full-dimensional observers which can not handle the uncertain parameters $\theta_C(t)$ and $\theta_L(t)$. In our design procedure, we utilize a reduced-order observer in the sampled-data form to avoid the hurdle caused by those uncertain nonlinear terms in system (3). The modified *output domination approach* [41] is used in the design where a tunable scaling gain is introduced to the compensator and controller to dominate the uncertain perturbing nonlinearities which are not exactly known. Moreover, since the sampled-data controller is dormant during the sampling instants, it may not effectively restrain the states between two neighbor sampling points, i.e., the famous *separation principle* is out of reach in this situation. To overcome this obstacle, a delicate stability analysis process is presented to show that, by carefully selecting the design gains and the tunable sampling period, the states of the system will globally asymptotically tend to the equilibrium even though we only change the control input values at the sampling points t_k.

Remark 3.3: From the design procedure, we should first choose the sampled-data observer gains N, and then the scaling gain M can be fixed. By the formulas (27), it seems that we can choose N and M to be arbitrary large. However, one can observe from (27) and (28) that the relation between the allowable tunable sampling period T and the scaling gain M can be represented as follows:

$$T < \frac{1}{\gamma M} \ln\left(1 + \frac{M - d_1 - d_5}{d_6 M N^2 \bar{\gamma}}\right) \tag{33}$$

which implies that the allowable sampling period T may be more conservative while M is increasing. On the other hand, numbers of nonlinear mathematical calculations and estimations for better neatness are included in the design procedure, and some guidelines on how to choose the gains M, N, β_1, β_2 have been given, but frankly speaking, the selection guidelines (27) and (28) are somewhat conservative. Hence in the practical application, the parameters are not necessarily required to be as large as those values determined by the sufficient conditions.

IV. Numerical Simulations and Experimental Results

In this section, numerical simulations and experiments results are shown in this section to illustrate the performance of the closed-loop system under the proposed sampled-data output feedback control law.

A. Numerical Simulations

The involved components values are selected as shown in Table I, the load resistance is set to be $R = 10(\Omega)$ and the uncertain parameters $\theta_L(t), \theta_C(t)$ in system (3) are assumed to be formulated by $\theta_L(t) = \theta_C(t) = \frac{3}{2} + \frac{1}{2}\sin(10t)$ and the step size taken is 0.01s. Fig. 3 shows the closed-loop performance under the sampled-data output feedback control law (5). It can be observed from the dynamic response curves that the controller performs well in the presence of those uncertain parameters, and high-efficient tracking task can also be achieved. More specifically, Fig. 4 shows the error between the estimated discrete-time state $\hat{x}_2(kT)$ and the system state $x_2(t)$ (i.e., $\frac{dv_o}{dt}$). The proposed robust reduced-order observer performs nice

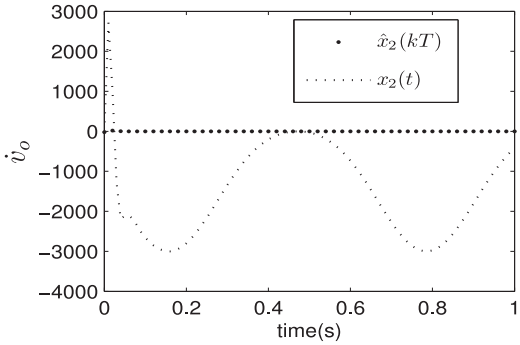

Fig. 4. Response curves of the estimated sampled-data state $\hat{x}_2(kT)$ and the system state $x_2(t)$ with the presence of uncertain parameters.

TABLE I
COMPONENTS VALUES OF THE DC–DC BUCK CONVERTER

Descriptions	Parameters	Nominal Values
Input Voltage	V_{in}	30 (V)
Desired Output Voltage	V_d	15 (V)
Inductance	L_0	4.7 (mH)
Capacitance	C_0	1000 (μF)

uncertainties attenuation, while the system state $x_2(t)$ is suffering from the involved components's periodically changing. In this simulation, the control parameters in the sampled-data controller (5) are selected as $\beta_1 = 2.0, \beta_2 = 1.0 \times 10^{-5}, M = 50, N = 1.5$, and the sampling period is set to be $T = 0.02$s.

Next, we show by simulation results that different closed-loop performances are related to different choices of sampling period T with the same selection of other control parameters. Fig. 5 compares the performance of the closed-loop dc–dc buck system under the proposed sampled-data output feedback control law (4) and (5) with three choices of $T = 0.02$s (the solid line), 0.1s (the dashed line), 1s (the dotted line), respectively. It is clear that the dynamic response performance of the hybrid closed-loop system becomes worse when the sampling period T changes from 0.02 to 0.1s but still effective to achieve the desired output values. When T is selected to be $T = 1$s, the output voltage fails to achieve the desired value $V_d = 15$(V) which indicates that $T = 1$s has exceeded the boundary of allowable sampling periods. The time history of the sampled-data duty ratio $\mu(t)$ is shown in Fig. 6.

Utilizing the linear control theory, one can easily construct the following linear continuous-time full-order observer designed for system (3) without consideration of the parameter uncertainties

$$\begin{aligned}\dot{\hat{x}}_1(t) &= \hat{x}_2(t) - a_1(\hat{x}_1(t) - x_1(t)) \\ \dot{\hat{x}}_2(t) &= \frac{1}{L_0 C_0}(\mu(t)V_{\text{in}} - V_d) - \frac{1}{L_0 C_0}\hat{x}_1(t) \\ &\quad - \frac{1}{C_0 R}\hat{x}_2(t) - a_2(\hat{x}_1(t) - x_1(t)) \end{aligned} \tag{34}$$

where $a_1 > 0, a_2 > 0$, hence the continuous-time PD output feedback controller can be designed as

$$\mu(t) = (V_d - k_1\hat{x}_1(t) - k_2\hat{x}_2(t))/V_{\text{in}} \tag{35}$$

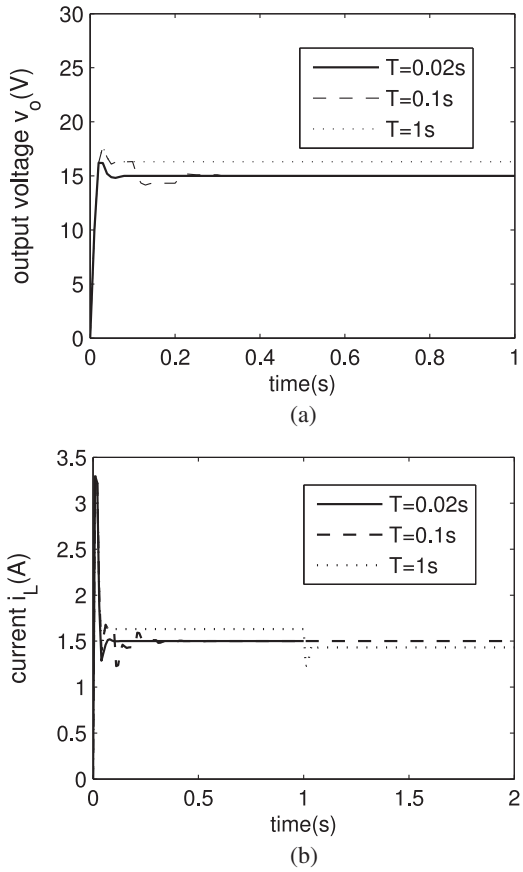

Fig. 5. Response curves of the system states under sampled-data output control law (5) with $T = 0.02$s (the solid line), $T = 0.1$s (the dashed line) and $T = 1s$ (the dotted line). (a) Output voltage v_o. (b) Current i_L.

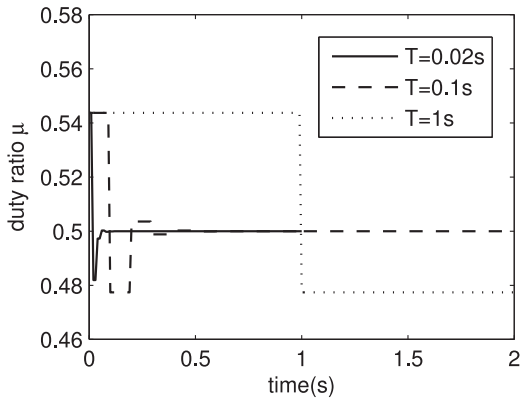

Fig. 6. Time history of the sampled-data control signal, duty ratio $\mu(t)$.

where k_1 and k_2 are positive constants. In what follows, we compare the control performances between the proposed sampled-data output feedback control law (5) and the PD type output feedback controller (35). By spending time on regulating the control parameters for these two controllers to make the performances of the closed-loop systems as good as possible for the sake of fair comparison. In this simulation, we set the uncertain parameter $\theta_L(t) = \theta_C(t) = \frac{55}{2} + \frac{53}{2}\sin(10t)$ for clear affection, and the control parameters are assigned to be $\beta_1 = 1.0, \beta_2 = 1.5 \times 10^{-6}, M = 50, N = 1.5$, $T = 0.02$s for

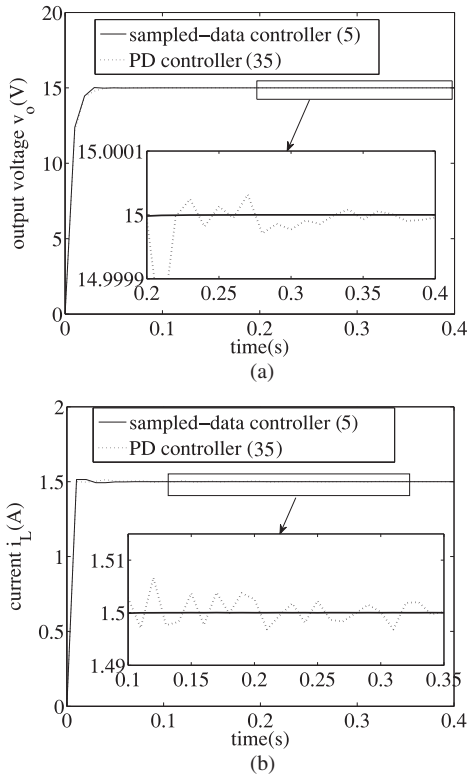

Fig. 7. Response curves of the system states comparison under sampled-data output control law (5) (the solid line) and PD output feedback control law (35) (the dotted line): (a) the output voltage v_o, (b) the current i_L.

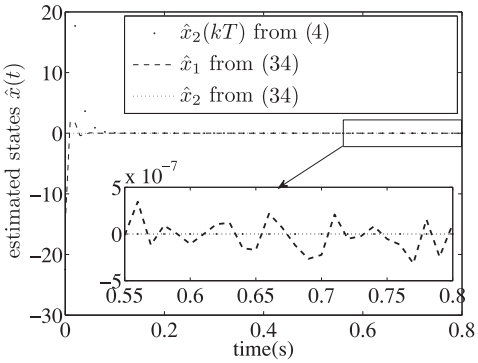

Fig. 8. Estimated states comparison between the robust sampled-data reduced-order observer (4) and the continuous-time full-order observer (34).

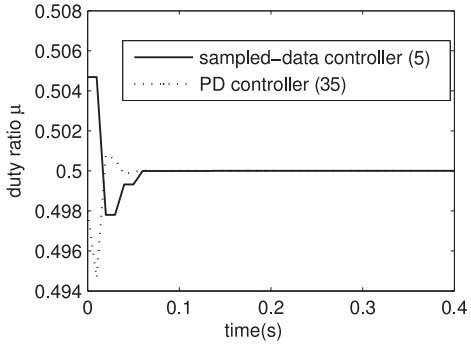

Fig. 9. Time history of the control signal, duty ratio $\mu(t)$: sampled-data output feedback control law (5) (the solid line), PD output feedback control law (35) (the dotted line).

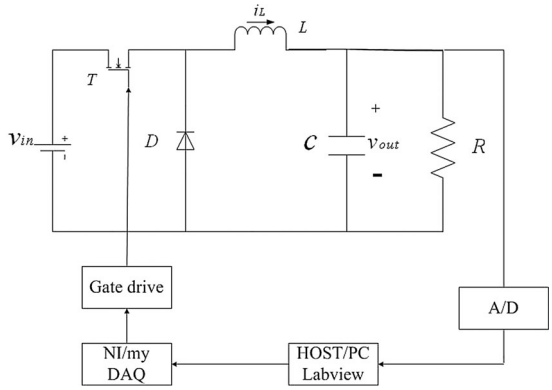

Fig. 10. Configuration of the experimental system.

Fig. 11. Experimental test setup.

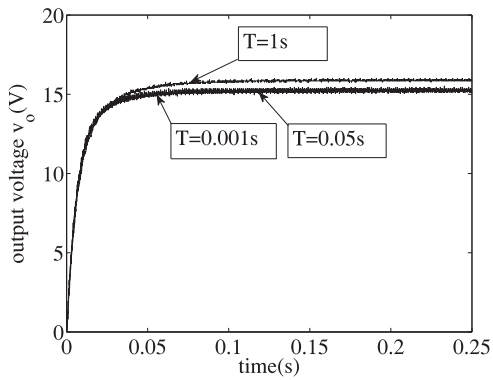

Fig. 12. Experimental behavior of the output voltage v_o under sampled-data output control law (5) with $T = 0.001$s, $T = 0.05$s and $T = 1$s.

the proposed sampled-data output feedback controller (4) and (5), $a_1 = 1, a_2 = 5, k_1 = 0.03, k_2 = 0.0005$ for the PD output feedback controller (34) and (35), respectively. The tracking control performances of the output voltage v_o and the current i_L between these two controllers are shown in Fig. 7. The estimated system states information $\hat{x}_2(kT)$ from the sampled-data reduced-order observer (4) (the solid line) and $\hat{x}_1(t), \hat{x}_2(t)$ from the continuous-time full-order observer (34) (the dotted line) is shown in Fig. 8. It is obvious that the time responding curves of the output voltage v_o and current i_L under both controllers are much similar since their state feedback control laws utilize the same PD type control method. But from the magnified part in Figs. 7 and 8, one can see clearly that the sampled-data output

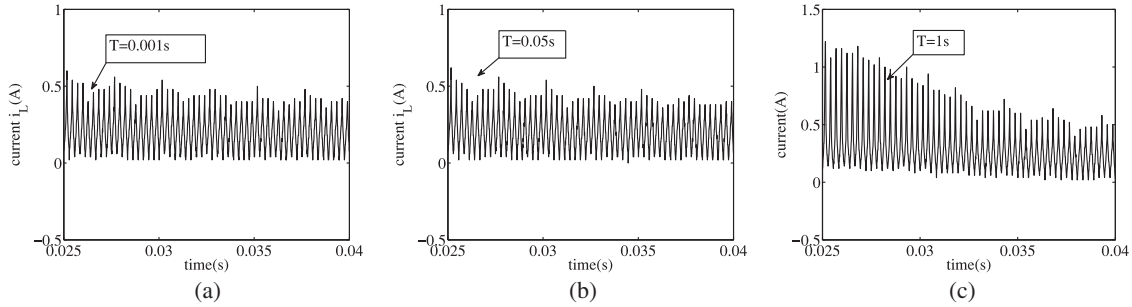

Fig. 13. Experimental behavior of the current i_L under sampled-data output control law (5) with $T = 0.001$s (a), $T = 0.05$s (b) and $T = 1$s (c).

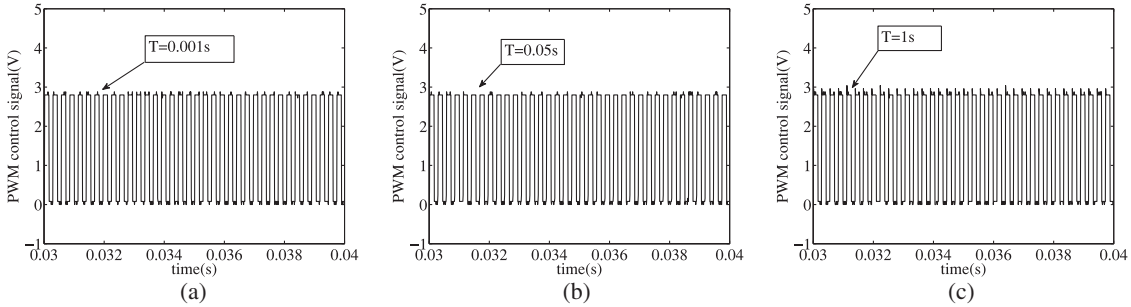

Fig. 14. Experimental time history of the PWM control signal (5) with $T = 0.001$s (a), $T = 0.05$s (b) and $T = 1$s (c).

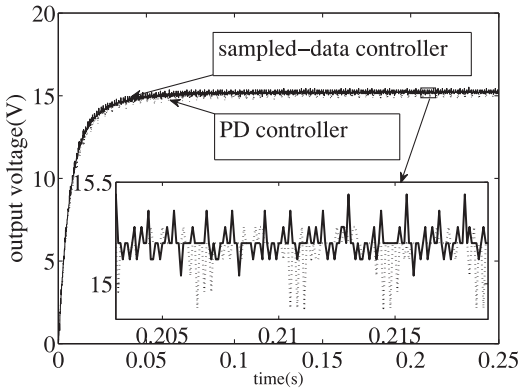

Fig. 15. Experimental behavior of the system states comparison under sampled-data output control law (5)(solid line) and PD output feedback control law (35)(dotted line).

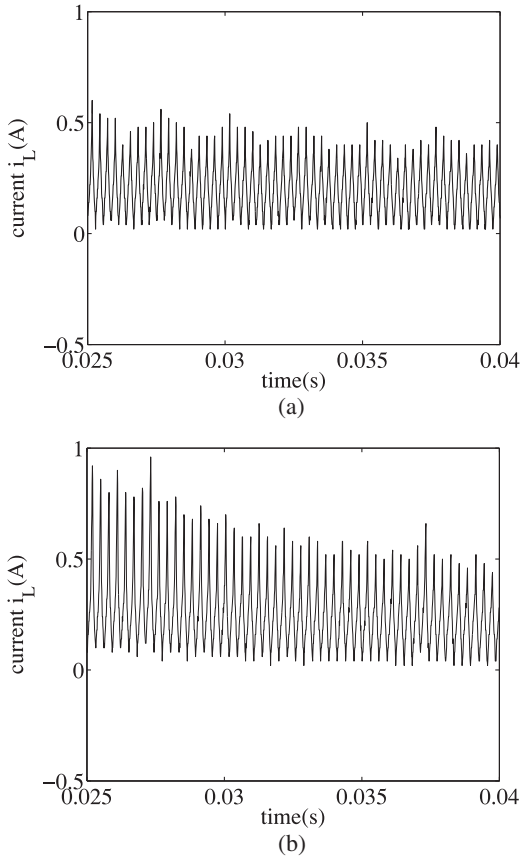

Fig. 16. (a) Experimental behavior of the current i_L under sampled-data output control law (5), and (b) PD output feedback control law (35) .

feedback controller proposed in this paper performs much better steady-state robustness in the presence of perturbations from components uncertainties due to the effectiveness of the robust sampled-data observer designed in this paper. As one can observe from Fig. 9, the control amplitudes of both control laws (5) (the solid line), (35) (the dotted line) are almost in the same level.

B. Experimental Results

To evaluate the performance of the proposed method, the experimental setup system for the proposed sampled-data output feedback control law has been built. The configuration and experimental test setup are shown in Figs. 10 and 11, respectively. The nominal values of the involved electronic components are shown in Table I and the load resistance in the experiment is

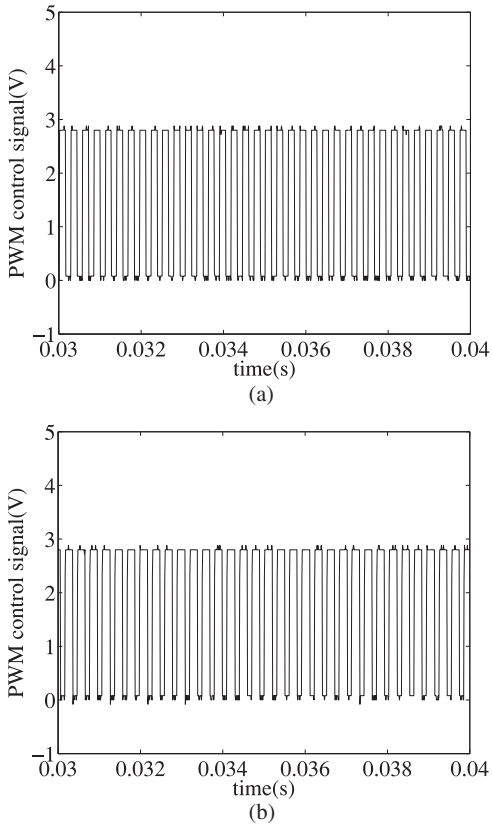

Fig. 17. (a) Experimental time history of the PWM control signal (5) and (b) PD output feedback control law (35).

chosen as $R = 100(\Omega)$. The control algorithm is implemented using a Labview program. In the following experiments, the control parameters in the sampled-data controller (5) are selected the same with $\beta_1 = 1, \beta_2 = 0.001, M = 2, N = 2.3$, and the switching frequency is set to be 3.6kHZ.

Figs. 12 and 13 show us the experimental behavior of the output voltage v_o under sampled-data output control law (5) with different choices of the sampling period $T = 0.001$, 0.05, and 1s, respectively. The time history of the PWM control signal is shown in Fig. 14. One can clearly observe that both the simulation and experimental results have consistent illustrations of the relationship between the closed-loop system performance and different choices of the sampling period T.

In what follows, we use experimental results to compare the control performances between the proposed sampled-data output feedback control law (4) and (5) and the continuous-time PD type output feedback controller (34) and (35) in which the parameters are selected as $a_1 = 1, a_2 = 5, k_1 = 0.01, k_2 = 0.005$. From Figs. 15 and 16, we observe that the steady-state error of the closed-loop system under sampled-data output feedback controller is smaller than that under the PD controller while both control amplitudes are almost in the same level as one can observe from Fig. 17.

V. Conclusion

This paper studies the global sampled-data output feedback control problem for the uncertain dc–dc buck power converters. By utilizing a sampled-data reduced-order observer to deal with the unknown parameters, a robust sampled-data output feedback control law has been developed to achieve global tracking control performance in high precision for dc–dc buck converters. Sampled-data control will give support to easier and cheaper implementation and hence is of significance in both theoretical and practical point of view. Numerical simulations and experimental results show the effectiveness of the proposed method.

Appendix

First, we list the following lemmas which play key roles in the proof of the main theorem.

Lemma A.1: Given any positive smooth function $\pi(x, y)$, the following holds:

$$|x||y| \le \frac{1}{2}\pi(x,y)|x|^2 + \frac{1}{2}\pi^{-1}(x,y)|y|^2.$$

Proof: It can be easily proved by completing the square and hence the details are omitted here. ■

Lemma A.2: [45] **(Gronwall-Bellman Inequality)** For real continuous functions $\eta(t), \alpha(t)$, and $\beta(t) \ge 0$ defined in a real region $\mathbb{D} := [a, b] \subset \mathbb{R}$, if $\eta(t)$ satisfies the following inequality:

$$\eta(t) \le \alpha(t) + \int_a^t \beta(s)\eta(s)ds,$$

the following holds for $t \in \mathbb{D}$:

$$\eta(t) \le \alpha(t) + \int_a^t \alpha(s)\beta(s)e^{\int_s^t \beta(r)dr}ds.$$

Second, the following part collects the detailed proofs of the propositions.

Proof of Proposition 3.1: By Assumption 2.1 and (20), one can obtain

$$\begin{aligned}
&\theta_L(t)\theta_C(t)\frac{M}{L_0C_0}|e(t)||u(t)| \\
&\le \frac{\bar\theta_L\bar\theta_C M}{L_0C_0}\beta_2\beta_1|e(t)|\big(|\hat x_2(t_k)| + |y(t_k)|\big) \\
&\le \frac{\bar\theta_L\bar\theta_C M}{L_0C_0}\beta_2\beta_1|e(t)|\big(|\hat x_2(t) - \hat x_2(t_k)| + |\hat x_2(t) - x_2(t)| \\
&\quad + |x_2(t)| + |y(t) - y(t_k)| + |y(t)|\big) \\
&\le \frac{\bar\theta_L\bar\theta_C M}{L_0C_0}\beta_2\beta_1|e(t)|\big(|\hat z(t) - \hat z(t_k)| + (N+1)|y(t) - y(t_k)| \\
&\quad + |e(t)| + |x_2(t)| + |y(t)|\big) \\
&\le + \frac{\bar\theta_L\bar\theta_C M}{L_0C_0}\beta_2\beta_1 e^2(t) + \frac{\bar\theta_L\bar\theta_C M}{L_0C_0}\beta_2\beta_1|e(t)|\big(|x_2(t)| + |y(t)|\big) \\
&\quad + \frac{\bar\theta_L\bar\theta_C M}{L_0C_0}(N+1)\beta_2\beta_1|e(t)| \cdot \|\mathcal{Z}(t) - \mathcal{Z}(t_k)\|,
\end{aligned}$$

$t \in [t_k, t_{k+1})$. (B.1)

From the definition of $\xi_2 = x_2 - x_2^* = x_2 + \beta_1\xi_1$, applying Lemma A.1, the following inequality can be concluded:

$$\begin{aligned}
&\frac{\bar{\theta}_L\bar{\theta}_C M}{L_0C_0}\beta_2\beta_1|e(t)|\big(|x_2(t)| + |y(t)|\big)\\
&= \frac{\bar{\theta}_L\bar{\theta}_C M}{L_0C_0}\beta_2\beta_1|e(t)|\big(|\xi_2(t)| + (\beta_1+1)|\xi_1(t)|\big)\\
&\le \frac{M}{8}(\xi_1^2(t) + \xi_2^2(t)) + M\tilde{d}_3e^2(t) \qquad \text{(B.2)}
\end{aligned}$$

where $\tilde{d}_3 > 0$ is a constant. Hence, (B.1) becomes

$$\begin{aligned}
&\theta_L(t)\theta_C(t)\frac{M}{L_0C_0}|e(t)\|u(t)|\\
&\le \frac{M}{8}(\xi_1^2(t) + \xi_2^2(t)) + M\tilde{d}_3|e(t)|^2\\
&\quad + \tilde{d}_4MN|e(t)|\cdot\|\mathcal{Z}(t) - \mathcal{Z}(t_k)\|, t\in[t_k, t_{k+1}) \qquad \text{(B.3)}
\end{aligned}$$

with a constant $\tilde{d}_4 > 0$.

From (18), (20), and Assumption 2.1, applying Lemma A.1, we have

$$\begin{aligned}
&\frac{M\theta_L(t)\theta_C(t)}{L_0C_0}|\xi_2(t)\|u(t) - u_c(t)|\\
&\le \frac{M\bar{\theta}_L\bar{\theta}_C}{L_0C_0}|\xi_2(t)|(\beta_2|x_2(t) - \hat{x}_2(t_k)| + \beta_1\beta_2|y(t) - y(t_k)|)\\
&\le \frac{M\bar{\theta}_L\bar{\theta}_C}{L_0C_0}|\xi_2(t)|\Big(\beta_2(|e(t)| + |\hat{z}(t) - \hat{z}(t_k)|)\\
&\quad + \beta_2(\beta_1 + N)|y(t) - y(t_k)|\Big)\\
&\le \frac{M}{8}\xi_2^2(t) + M\bar{d}_3e^2(t) + \bar{d}_4MN|\xi_2(t)|\cdot\|\mathcal{Z}(t) - \mathcal{Z}(t_k)\|,\\
&t\in[t_k, t_{k+1}) \qquad \text{(B.4)}
\end{aligned}$$

where $\bar{d}_3 > 0$, $\bar{d}_4 > 0$ are two constants.

Combing (B.3) and (B.4) yields

$$\begin{aligned}
&\theta_L(t)\theta_C(t)\frac{M}{L_0C_0}|e(t)\|u(t)| + \frac{M\theta_L(t)\theta_C(t)}{L_0C_0}|\xi_2(t)\|u(t) - u_c(t)|\\
&\le \frac{M}{4}(\xi_1^2(t) + \xi_2^2(t)) + Md_3e^2(t)\\
&+ d_4MN(|\xi_2(t)| + |e(t)|)\cdot\|\mathcal{Z}(t) - \mathcal{Z}(t_k)\|, t\in[t_k, t_{k+1}) \qquad \text{(B.5)}
\end{aligned}$$

with constants $d_3 = \tilde{d}_3 + \bar{d}_3$ and $d_4 = \tilde{d}_4 + \bar{d}_4$.

Proof of Proposition 3.2: Denote the hybrid closed-loop system (6), (2), and (20) to be $\dot{\mathcal{Z}}(t) = \Psi\big(M, \mathcal{Z}(t_k), \mathcal{Z}(t)\big)$. The following inequality holds for a constant $\gamma > 0$:

$$\begin{aligned}
&\|\mathcal{Z}(t) - \mathcal{Z}(t_k)\|\\
&\le \int_{t_k}^{t}\|\Psi\big(M, \mathcal{Z}(t_k), \mathcal{Z}(s)\big)\|ds\\
&\le \int_{t_k}^{t}\gamma M\big(\|\mathcal{Z}(s) - \mathcal{Z}(t_k)\| + \|\mathcal{Z}(t_k)\|\big)ds\\
&\le \gamma M(t - kT)\|\mathcal{Z}(t_k)\| + \int_{t_k}^{t}\gamma M\|\mathcal{Z}(s) - \mathcal{Z}(t_k)\|ds,\\
&t\in[t_k, t_{k+1}).
\end{aligned}$$

Applying Lemma A.2, one can obtain

$$\begin{aligned}
&\|\mathcal{Z}(t) - \mathcal{Z}(t_k)\|\\
&\le \gamma M(t - kT)\|\mathcal{Z}(t_k)\| + \gamma^2M^2\|\mathcal{Z}(t_k)\|\\
&\quad\times\int_{kT}^{t}(s - kT)e^{\gamma M(t-s)}ds,\\
&\le \|\mathcal{Z}(t_k)\|\left(e^{\gamma M(t-kT)} - 1\right)\\
&\le \bar{\gamma}\sqrt{U(\mathcal{Z}(t_k))}\left(e^{\gamma M(t-kT)} - 1\right), t\in[t_k, t_{k+1}) \qquad \text{(B.6)}
\end{aligned}$$

where $\bar{\gamma} > 0$ is a constant.

REFERENCES

[1] D. Montesinos-Miracle, M. Massot-Campos, J. Bergas-Jane, S. Galceran-Arellano, and A. Rufer, "Design and control of a modular multilevel DC/DC converter for regenerative applications," *IEEE Trans. Power Electron.*, vol. 28, no. 8, pp. 3970–3979, Aug. 2013.

[2] R. Retegui, M. Benedetti, M. Funes, P. Antoszczuk, and D. Carrica, "Current control for high-dynamic high-power multiphase buck converters," *IEEE Trans. Power Electron.*, vol. 27, no. 2, pp. 614–618, Feb. 2012.

[3] O. Garcia, M. Vasić, P. Alou, J. Oliver, and J. Cobos, "An overiew of fast DC–DC converters for envelope amplifier in RF transmitters," *IEEE Trans. Power Electron.*, vol. 28, no. 10, pp. 4712–4722, Oct. 2013.

[4] Z. Qian, O. Abdel-Rahman, H. Al-Atrash, and I. Batarseh, "Modeling and control of three-port DC/DC converter interface for satellite applications," *IEEE Trans. Power Electron.*, vol. 25, no. 3, pp. 637–649, Mar. 2010.

[5] S. J. Amodeo, H. G. Chiacchiarini, and A. R. Oliva, "High-performance control of a DC-DC z-source converter used for an excitation field driver," *IEEE Trans. Power Electron.*, vol. 27, no. 6, pp. 2947–2957, Jun. 2012.

[6] E. Serban and H. Serban, "A control strategy for a distributed power generation microgrid application with voltage-and current-controlled source converter," *IEEE Trans. Power Electron.*, vol. 25, no. 12, pp. 2981–2992, Dec. 2010.

[7] C.-S. Chiu, Y.-L. Ouyang, and C.-Y. Ku, "Terminal sliding mode control for maximum power point tracking of photovoltaic power generation systems," *Sol. Energy*, vol. 86, pp. 2986–2995, 2012.

[8] W. Chen, A. Q. Huang, C. Li, G. Wang, and W. Gu, "Analysis and comparison of medium voltage high power dc/dc converters for offshore wind energy systems," *IEEE Trans. Power Electron.*, vol. 28, no. 4, pp. 2014–2023, Apr. 2013.

[9] E. Meyer, Z. Zhang, and Y.-F. Liu, "Controlled auxiliary circuit to improve the unloading transient response of buck converters," *IEEE Trans. Power Electron.*, vol. 25, no. 4, pp. 806–819, Apr. 2010.

[10] L. Wang, Y. Pei, X. Yang, Y. Qin, and Z. Wang, "Improving light and intermediate load efficiencies of buck converters with planar nonlinear inductors and variable on time control," *IEEE Trans. Power Electron.*, vol. 27, no. 1, pp. 342–353, Jan. 2012.

[11] R. D. Middlebrook and S. Cuk, "A general unified approach to modelling switching-converter power stages," in *Proc. Power Electron. Spec. Conf.*, 1976, vol. 1, pp. 18–34.

[12] J. Alvarez-Ramirez, G. Espinosa-Pérez, and D. Noriega-Pineda, "Current-mode control of DC–DC power converters: A backstepping approach," *Int. J. Robust Nonlinear Control*, vol. 13, no. 5, pp. 421–442, 2003.

[13] H. El Fadil, F. Giri, O. El Magueri, and F. Chaoui, "Control of DC–DC power converters in the presence of coil magnetic saturation," *Contr. Eng. Pract.*, vol. 17, no. 7, pp. 849–862, 2009.

[14] S.-C. Tan, Y.-M. Lai, C. K. Tse, and M. K. Cheung, "Adaptive feedforward and feedback control schemes for sliding mode controlled power converters," *IEEE Trans. Power Electron.*, vol. 21, no. 1, pp. 182–192, Jan. 2006.

[15] P. Karamanakos, T. Geyer, and S. Manias, "Direct voltage control of dc-dc boost converters using enumeration-based model predictive control," *IEEE Trans. Power Electron.*, vol. 29, no. 2, pp. 968–978, Feb. 2014.

[16] Y. He and F. L. Luo, "Sliding-mode control for DC–DC converters with constant switching frequency," *IEE Proc.-Control Theory Appl.*, vol. 153, no. 1, pp. 37–45, 2006.

[17] S.-C. Tan, Y.-M. Lai, and C. K. Tse, "General design issues of sliding-mode controllers in DC–DC converters," *IEEE Trans. Ind. Electron.*, vol. 55, no. 3, pp. 1160–1174, Mar. 2008.

[18] S.-C. Tan, Y.-M. Lai, and C. K. Tse, *Sliding Mode Control of Switching Power Converters*. Boca Raton, FL, USA: CRC Press, 2011.
[19] H. Komurcugil, "Non-singular terminal sliding-mode control of DC–DC buck converters," *Control Eng. Pract.*, vol. 21, no. 3, pp. 321–332, 2012.
[20] C. Elmas, O. Deperlioglu, and H. H. Sayan, "Adaptive fuzzy logic controller for DC–DC converters," *Expert Syst. Appl.*, vol. 36, no. 2, pp. 1540–1548, 2009.
[21] D. Cao, S. Jiang, and F. Z. Peng, "Optimal design of multilevel modular capacitor-clamped DC–DC converter," *IEEE Trans. Power Electron.*, vol. 28, no. 8, pp. 3816–3826, Aug. 2013.
[22] E. Meyer, Z. Zhang, and Y.-F. Liu, "An optimal control method for buck converters using a practical capacitor chargebalance technique," *IEEE Trans. Power Electron.*, vol. 23, no. 4, pp. 1802–1812, Jul. 2008.
[23] M. M. Peretz and S. Ben-Yaakov, "Time-domain design of digital compensators for pwm dc-dc converters," *IEEE Trans. Power Electron.*, vol. 27, no. 1, pp. 284–293, Jan. 2012.
[24] M. Musallam, P. P. Acarnley, C. M. Johnson, L. Pritchard, and V. Pickert, "Power electronic device temperature estimation and control in pulsed power and converter applications," *Control Eng. Pract.*, vol. 16, no. 12, pp. 1438–1442, 2008.
[25] Y. Han, G. Cheung, A. Li, C. R. Sullivan, and D. J. Perreault, "Evaluation of magnetic materials for very high frequency power applications," *IEEE Trans. Power Electron.*, vol. 27, no. 1, pp. 425–435, Jan. 2012.
[26] W. Alexander, *Uncertain Models and Robust Control*. New York, NY, USA: Springer-Verlag, 1991.
[27] S. Li and Z. Liu, "Adaptive speed control for permanent-magnet synchronous motor system with variations of load inertia," *IEEE Trans. Ind. Electron.*, vol. 56, no. 8, pp. 3050–3059, Aug. 2009.
[28] J. Yang, S. Li, and X. Yu, "Sliding-mode control for systems with mismatched uncertainties via a disturbance observer," *IEEE Trans. Ind. Electron.*, vol. 60, no. 1, pp. 160–169, Jan. 2013.
[29] S. Chattopadhyay and S. Das, "A digital current-mode control technique for DC–DC converters," *IEEE Trans. Power Electron.*, vol. 21, no. 6, pp. 1718–1726, Nov. 2006.
[30] M. Aime, G. Gateau, and T. A. Meynard, "Implementation of a peak-current-control algorithm within a field-programmable gate array," *IEEE Trans. Ind. Electron.*, vol. 54, no. 1, pp. 406–418, Feb. 2007.
[31] P. Midya, P. Krein, and M. Greuel, "Sensorless current mode control-an observer-based technique for dc-dc converters," *IEEE Trans. Power Electron.*, vol. 16, no. 4, pp. 522–526, Jul. 2001.
[32] F. Giri, O. El Maguiri, H. El Fadil, and F. Chaoui, "Nonlinear adaptive output feedback control of series resonant DC–DC converters," *Control Eng. Pract.*, vol. 19, no. 10, pp. 1238–1251, 2011.
[33] D. Nešić and A. R. Teel, "Sampled-data control of nonlinear systems: An overview of recent results," in *In Perspectives in Robust Control (Lecture Notes in Control and Information Science)*. vol. 268, New York, NY, USA: Springer-Verlag, 2001, pp. 221–239.
[34] B. Tang, Q. Zeng, D. He, and Y. Zhang, "Random stabilization of sampled-data control systems with nonuniform sampling," *Int. J. Autom. Comput.*, vol. 9, pp. 492–500, 2012.
[35] H. Du, C. Qian, and S. Li, "Global stabilization of a class of uncertain upper-triangular systems under sampled-data control," *Int. J. Robust Nonlinear Control*, vol. 23, no. 6, pp. 620–637, 2012.
[36] D. Nešić, A. R. Teel and D. Carnevale, "Explicit computation of the sampling period in emulation of controllers for nonlinear sampled-data systems," *IEEE Trans. Autom. Control*, vol. 54, no. 3, pp. 619–624, Mar. 2009.
[37] C. Qian and H. Du, "Global output feedback stabilization of a class of nonlinear systems via linear sampled-data control," *IEEE Trans. Autom. Control*, vol. 57, no. 11, pp. 2934–2939, Nov. 2012.
[38] C. Zhang, C. Qian, and S. Li, "Global decentralized control of interconnected nonlinear systems by sampled-data output feedback," in *Proc. Amer. Control Conf.*, 2013, pp. 6559–6564.
[39] C. Qian and W. Lin, "A continuous feedback approach to global strong stabilization of nonlinear systems," *IEEE Trans. Autom. Control*, vol. 46, no. 7, pp. 1061–1079, Jul. 2001.
[40] H. Du, C. Qian, S. Yang, and S. Li, "Recursive design of finite-time convergent observers for a class of time-varying nonlinear systems," *Automatica*, vol. 49, no. 2, pp. 601–609, 2013.
[41] C. Qian, "A homogeneous domination approach for global output feedback stabilization of a class of nonlinear systems," in *Proc. 2005 Amer. Control Conf.*, Jun. 2005, pp. 4708–4715.
[42] A. Isidori, *Nonlinear Control Systems*, Communications and Control Engineering Series), 3rd ed. Berlin, Germany: Springer-Verlag, 1995.
[43] A. M. Dabroom and H. K. Khalil, "Output feedback sampled-data control of nonlinear systems using high-gain observers," *IEEE Trans. Autom. Control*, vol. 46, no. 11, pp. 1712–1725, Nov. 2001.
[44] H. El Fadil and F. Girt, "Backstepping based control of PWM DC–DC boost power converters," in *Proc. IEEE Int. Symp. Ind. Electron.*, 2007, pp. 395–400.
[45] T. M. Apostol, *Mathematical Analysis*, 2nd ed. New York, NY, USA: Addison-Wesley, 1974.

Chuanlin Zhang was born in Jiangsu, China, in 1986. He received the B.S. degree in mathematics from Southeast University, Nanjing, China, in 2008, where he is currently working toward the Ph.D degree in the School of Automation, Southeast University.

His research interests include nonlinear system control, digital control for power electronic systems, and aircraft systems.

Junxiao Wang was born in Wuxue, Hubei Province, China, in 1986. He received the B.S. and M.S. degrees from Information Engineering College, Henan University of Science and Technology (HAUST), Luoyang, China, in 2008 and 2011, respectively. He is currently working toward the Ph.D. degree in control theory and control engineering from the School of Automation, Southeast University, Nanjing, China.

His research interests include advanced control theory and its application to power electronics and ac motor control systems.

Shihua Li (A'05–M'06–SM'10) was born in Pingxiang, Jiangxi, China, in 1975. He received the Bachelor's, Master's, and Ph.D. degrees all in automatic control from Southeast university, Nanjing, China in 1995, 1998, and 2001, respectively.

Since 2001, he has been with the School of Automation, Southeast University, where he is currently a professor. His main research interests include nonlinear control theory with applications to robot, spacecraft, ac motor, and other mechanical systems.

Bin Wu was born in Taian, Shandong Province, China, in 1990. He received the B.S. degree in automation from Anhui University, Hefei, China, in 2013. He is now working toward the M.S. degree from the School of Automation, Southeast University, Nanjing, China.

His research interests include control theory with applications to power electronics and ac motors.

Chunjiang Qian (S'98–M'01–SM'03) received the Ph.D. degree in electrical engineering from Case Western Reserve University, Cleveland, OH, USA, 2001.

Since August 2001, he has been with the Department of Electrical and Computer Engineering, The University of Texas at San Antonio, San Antonio, TX, USA, where he is currently a Professor. His current research interests include robust and adaptive control, nonlinear systems theory, optimal control, cyber-physical systems, flight control, and power plant control. In those areas, so far he has published more than 150 papers and coauthored one monograph.

Dr. Qian has received 2003 U.S. National Science Foundation (NSF) CAREER Award and one the Regents Outstanding Teaching Award, the University of Texas System, 2009. He received the third Best Paper Award in the ISA (International Society of Automation) Power Industry Division Symposium (2011) and the Best Poster Paper Award in the 3rd IFAC International Conference on Intelligent Control and Automation Science (2013). He currently serves as an Associate Editor for *Automatica* and a Subject Editor for *International Journal of Robust and Nonlinear Control*.